Rotational Diffusion of Nondipolar Probes in Triton X-100 Micelles: Role of Specific Interactions and Micelle Size on Probe Dynamics

G. B. Dutt*

Radiation Chemistry & Chemical Dynamics Division, Bhabha Atomic Research Centre, Trombay, Mumbai 400 085, India

Received: February 6, 2002; In Final Form: April 29, 2002

Temperature dependent rotational relaxation studies of two structurally similar nondipolar probes: 2,5-dimethyl-1,4-dioxo-3,6-diphenylpyrrolo[3,4-*c*]pyrrole (DMDPP) and 1,4-dioxo-3,6-diphenylpyrrolo[3,4-*c*]pyrrole (DPP), have been carried out in Triton X-100 micelles in an attempt to explore the influence of specific interactions and micellar size on the dynamics of probe molecules. The time-resolved anisotropy in micelles, decays as a sum of two exponentials with two time constants, one corresponding to a fast reorientation time and the other to a slow one, for both the probes over the entire range of temperature studied. The results are analyzed in terms of a two-step model consisting of fast-restricted rotation of the probe and slow lateral diffusion of the probe in the micelle that are coupled to the rotation of the micelle as a whole. However, as the temperature is raised, the size of the Triton X-100 micelles increase significantly and the measured slow reorientation time corresponds solely to the lateral diffusion of the probe in the micelle. This is because the reorientation time for the overall rotation of the micelle becomes very long and consequently the fluorescence depolarization due to this process becomes negligible. It has also been observed that the short and long components of the anisotropy decay for DPP are found to be considerably slower than the corresponding ones for DMDPP due to the strong hydrogen bonding interactions between the ethylene oxide groups of the surfactant units and the secondary amino groups of the probe.

1. Introduction

Rotational diffusion studies of solutes solubilized in micelles are essential to get a better insight into many chemical processes such as electron transfer, excitation energy transport, and photoisomerizaion reactions in organized media. Moreover, studies in micellar systems are also important, as they are akin to biological membranes. Time-resolved fluorescence depolarization method is one of the most powerful techniques to study the rotational diffusion of fluorescent probes in micelles. Over the years, a number of groups have studied the dynamics of probes solubilized in micelles, reverse micelles and polymer-surfactant aggregates by measuring the decay of anisotropy $r(t)$.[1−8] Although $r(t)$ of a majority of organic solutes in homogeneous solutions decays as single exponential[9] with one reorientation time τ_r, the anisotropy decay in micelles is complex and is often described by two exponentials. The reason for such biexponential behavior in micelles is due to the involvement of more than one kind of motion.

In a number of studies ionic probes were used,[1−3,5,6,8] and the idea behind choosing such probes is that they tend to locate near the surface of the micelle. But it has been fairly well established that practically all kinds of molecules have a surface-seeking tendency in the micelle and even the hydrophobic molecules prefer the interfacial region as the site for solubilization.[10,11] The most commonly employed surfactants are sodium dodecyl sulfate (SDS) with anionic headgroups, cetyltrimethylammonium bromide (CTAB), dodecyltrimethylammonium bromide (DTAB) with cationic headgroups, and the nonionic Triton X-100 (TX-100). It has been observed that anionic probes strongly interact with cationic micelles and vice versa due to electrostatic interactions, which has been reflected in the measured reorientation times. In almost all the earlier studies the micelles used, with the exception of TX-100, are comparatively smaller (micelle radius r_M in the range of 15−25 Å) in size. In the present investigation, however, experiments have been carried out in large TX-100 micelles in the temperature range of 283−323 K. The TX-100 micelles are known to grow in size (r_M goes up from 30 to 83 Å) upon rising the temperature in the above-mentioned range.[12] Thus the present work will enable us to understand how the size of the micelle effects the dynamics of the probe molecules.

Besides understanding the effect of micelle size on the probe dynamics, we also wish to investigate how the specific interactions between the probe and micelle influence the dynamics of the probe. For this purpose, we have studied the rotational diffusion of two structurally similar nondipolar probes: 2,5-dimethyl-1,4-dioxo-3,6-diphenylpyrrolo[3,4-*c*]pyrrole (DMDPP) and 1,4-dioxo-3,6-diphenylpyrrolo[3,4-*c*]pyrrole (DPP) (see Figure 1 for molecular structures of the probes), in TX-100 micelles as a function of temperature. In recent times, we have extensively studied the rotational dynamics of these probes in hydrogen bonding solvents[13−16] and in electrolyte solutions of dimethyl sulfoxide[17] with the idea of finding out how the presence and absence of specific interactions between the solute and the solvent effect the friction experienced by the solute molecule. The probe DPP was found to rotate 2−3 times slower than DMDPP due to specific interactions with the solvents. The specific interactions are between the two NH groups of DPP and the hydroxyl groups of the solvents. Since the TX-100 surfactant units possess ethylene oxide groups, the probe DPP is expected to strongly interact with them. Hence the study

* To whom correspondence should be addressed. E-mail: gbdutt@apsara.barc.ernet.in.

10.1021/jp0203447 CCC: $22.00
Published on Web 06/25/2002

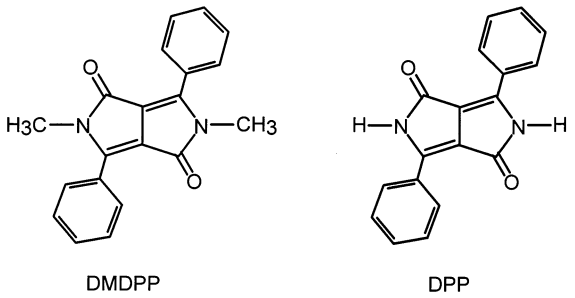

Figure 1. Molecular structures of the probes DMDPP and DPP.

undertaken here will help us explore how the rotational diffusion of hydrogen bonding probe DPP and nonhydrogen bonding probe DMDPP are effected in the micellar environment. The remainder of the paper is organized in the following manner. Section 2 describes the experimental methods used to measure the rotational diffusion of the probes in micelles. Results are presented in section 3, and they are discussed in terms of the two-step model in section 4. The conclusions are summarized in the last section.

2. Experimental Section

The probes DMDPP and DPP are from Ciba Specialty Chemicals Inc., Switzerland and the surfactant TX-100 is from BDH Chemicals Ltd., England. All these chemicals were of the highest available purity and were used as such. Double distilled water was used in the preparation of the micelle samples. The concentration of the surfactant was 40 mM. The probe molecules were dissolved in the micelle solutions by gentle heating in a water bath and it was ensured that the concentrations of the probes were in the range of $10^{-5}-10^{-6}$ M.

Steady-state anisotropies of the samples were measured using Hitachi F-4010 spectroflorimeter and the details have been described in our earlier publication.[13] The probes DMDPP and DPP were excited at 440 nm and the emission was monitored in the range of 515−585 nm. Time-resolved fluorescence depolarization measurements were carried out using time-correlated single-photon counting[18] facility at the Tata Institute of Fundamental Research, Mumbai. The excitation source is a diode pumped, intracavity doubled cw Nd:YAG laser that pumps a picosecond Ti:saphire laser (Tsunami, Spectra Physics). The frequency-doubled output of the laser was used to excite the samples. Details of the system have been described elsewhere.[14] Both the probes DMDPP and DPP were excited at 444 nm with a vertically polarized pulse and the fluorescence decays were collected at 550 nm by keeping the emission polarizer parallel $I_{||}(t)$, perpendicular $I_{\perp}(t)$, and also at the magic angle $I(t)$ (54.7°) with respect to the excitation polarization. For the parallel component of the decay, 20000 peak counts were collected and the perpendicular component of the decay was corrected for the polarization bias of the detection system or the *G*-factor of the spectrometer. A time increment of 85.4 ps/ch was used and the decays were collected in 512 channels. The decays measured in this manner were convoluted with the instrument response function, which was measured by replacing the sample with a solution that scatters light. Each measurement was repeated at least 2−3 times, and the average values are reported. In both the steady-state and time-resolved apparatus, the desired sample temperature was achieved with the help of a temperature controller, Eurotherm.

Fluorescence lifetime τ_f was obtained from the decays measured at magic angle polarization by iterative reconvolution method using Marquardt algorithm as described by Bevington.[19]

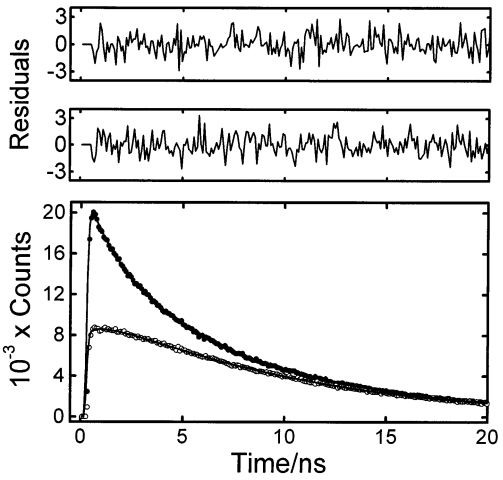

Figure 2. Experimentally measured $I_{||}(t)$ (filled circles) and $I_{\perp}(t)$ (open circles) curves of DMDPP in TX-100 micelles at 283 K. The lines passing through them are the fitted ones. The instrument response function is not shown in the figure for the sake of clarity. Although the total range of the abscissa is over 40 ns, only 20 ns were displayed in the figure in order to highlight the decay of $I_{||}(t)$ and $I_{\perp}(t)$ curves. The lower and upper panels represent the distribution of the weighted residuals for $I_{||}(t)$ and $I_{\perp}(t)$, respectively. The parameters obtained from the simultaneous analysis of $I_{||}(t)$ and $I_{\perp}(t)$ are listed in Table 1.

Similarly, the anisotropy decay parameters were obtained by a simultaneous fit[20,21] of $I_{||}(t)$ and $I_{\perp}(t)$ curves given by eqs 1 and 2.

$$I_{||}(t) = \frac{1}{3}I(t)[1 + 2r(t)] \quad (1)$$

$$I_{\perp}(t) = \frac{1}{3}I(t)[1 - r(t)] \quad (2)$$

It has been shown[5] that the anisotropy parameters are recovered more accurately if less number of parameters are optimized in the simultaneous fit. To reduce this number, the τ_f value obtained from the magic angle decay analysis was kept fixed, while performing the simultaneous fit. The goodness of the fit was judged by statistical parameters such as the reduced χ^2 being close to unity and the random distribution of the weighted residuals.

3. Results

Fluorescence decays of both the probes DMDPP and DPP in TX-100 micelles were adequately described by single-exponential function with one lifetime. The anisotropy decays of these probes in TX-100, however, followed a biexponentail function of the form

$$r(t) = r_0[\beta \exp(-t/\tau_{slow}) + (1 - \beta) \exp(-t/\tau_{fast})] \quad (3)$$

where r_0 is the initial anisotropy and τ_{slow} and τ_{fast} are the two reorientation times. The significance of the subscripts "slow" and "fast" will become evident when we discuss the two-step model in the next section. To represent the goodness of the fits, $I_{||}(t)$ and $I_{\perp}(t)$ curves for DMDPP and DPP in TX-100 micelles at 283 K, together with the residual distributions are shown the in Figures 2 and 3, respectively. Likewise, the fluorescence lifetimes and the anisotropy decay parameters for DMDPP and DPP are given in Tables 1 and 2, respectively. It can be seen from the tables that the fluorescence lifetimes are around 8.75 ns for DMDPP and 6.90 ns for DPP. There is only a marginal decrease in the lifetimes of both the probes with an

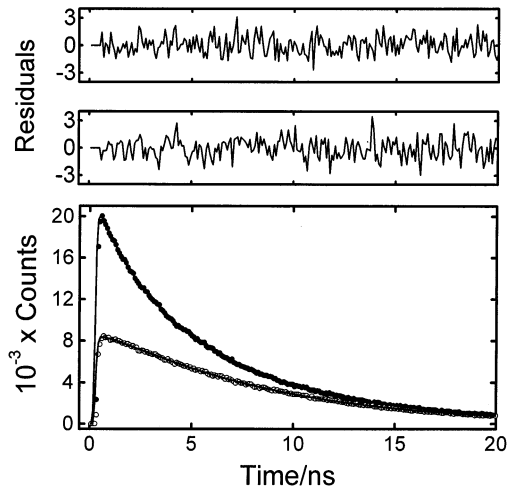

Figure 3. Experimentally measured $I_{||}(t)$ (filled circles) and $I_{\perp}(t)$ (open circles) curves of DPP in TX-100 micelles at 283 K. The lines passing through them are the fitted ones. The instrument response function is not shown in the figure for the sake of clarity. Although the total range of the abscissa is over 40 ns, only 20 ns were displayed in the figure in order to highlight the decay of $I_{||}(t)$ and $I_{\perp}(t)$ curves. The lower and upper panels represent the distribution of the weighted residuals for $I_{||}(t)$ and $I_{\perp}(t)$, respectively. The parameters obtained from the simultaneous analysis of $I_{||}(t)$ and $I_{\perp}(t)$ are listed in Table 2.

increase in the temperature. The r_0 values obtained from the analyses are lower than the measured values by 7%−13% and 4%−9%, respectively, for DMDPP and DPP, while the corresponding r_0 values that were measured using the steady-state depolarization method in glucose glass[13] are 0.364 ± 0.006 and 0.362 ± 0.004. The ratios of τ_{slow} to τ_{fast} for DMDPP and DPP are 3−5 and 4−5, respectively. To compare the anisotropy decays of DMDPP and DPP in TX-100 micellar solutions, the average reorientation time $\langle\tau_r\rangle$, which is a model independent parameter, is defined using the following relation.

$$\langle\tau_r\rangle = \beta\tau_{slow} + (1-\beta)\tau_{fast} \tag{4}$$

The values calculated using eq 4 for DMDPP and DPP are given in column 7 of Tables 1 and 2, respectively. It can be inferred from these tables that the $\langle\tau_r\rangle$ values of DPP are longer than those of DMDPP by 65%−110%. To illustrate this fact, the anisotropy decays of DMDPP and DPP at 283 and 323 K together with the fitted curves are shown in Figure 4. It is visually obvious from the plots of the figure that the $\langle\tau_r\rangle$ values of DPP are significantly longer than that of DMDPP at 283 K as well as at 323 K.

To see how well the recovered anisotropy parameters match with the "true values", the experimentally measured steady-state anisotropies are compared with the steady-state anisotropies calculated using the anisotropy parameters obtained from the fits. The steady-state anisotropy $\langle r\rangle$ is defined[22] as the average of $r(t)$ weighted by $I(t)$ using the relation

$$\langle r\rangle = \frac{\int_0^\infty r(t)I(t)\,dt}{\int_0^\infty I(t)\,dt} \tag{5}$$

$\langle r\rangle$ can be evaluated by integration of eq 5 after substituting the appropriate expressions for $I(t)$ and $r(t)$, and the resulting expression is given by

$$\langle r\rangle = r_0\left[\frac{\beta\tau_{slow}}{(\tau_f+\tau_{slow})} + \frac{(1-\beta)\tau_{fast}}{(\tau_f+\tau_{fast})}\right] \tag{6}$$

The $\langle r\rangle$ values calculated with the help of eq 6 using the anisotropy parameters and the ones measured using steady-state depolarization method are also given in Tables 1 and 2 for DMDPP and DPP, respectively. The agreement between the $\langle r\rangle$ values obtained using both the methods is within 12% in most of the cases and between 15% and 20% in a few other cases. This kind of agreement seems quite reasonable considering the fact that a good number of parameters are optimized in the analysis. This exercise confirms that the anisotropy parameters recovered from the analysis are close to the true values.

4. Discussion

Before we discuss the rotational diffusion of the probes DMDPP and DPP in TX-100 micelles, it is worthwhile to briefly discuss the results obtained for these probes in homogeneous solutions. Majority of the rotational diffusion studies involving DMDPP and DPP have been carried out[13−17] using steady-state fluorescence depolarization method with the assumption that decay of anisotropy is single exponential. This assumption is justified because multiexponential anisotropy decays are observed only for those solute molecules having a high degree of symmetry and not possessing any freely rotating groups: anthracene, perylene, and triphenylene are some of the examples.[23] Moreover, we have also carried out time-resolved anisotropy experiments of these probes in glycerol[14] at several temperatures. These studies revealed that the anisotropy decays of DMDPP and DPP are indeed single exponentials. The important finding from our studies on these probes is that the solute−solvent hydrogen bonding significantly hinders molecular rotation. As mentioned in the Introduction, DPP because of its two NH groups is capable of forming hydrogen bonds with the hydroxyl groups of the solvents and was found to rotate 2−3 times slower than DMDPP in solvents such as alcohols, ethylene glycol and glycerol. On the other hand, DMDPP, in which two $N-CH_3$ groups replace the two NH groups, behaves like any other nonpolar solute and its reorientation times are sensitive to the size of the solvent. In other words, as the size of the solvent increases, the friction experienced by the solute molecule decreases.[24,25] In one of our recent papers,[17] where rotational dynamics studies of DMDPP and DPP have been carried out in electrolyte solutions of dimethyl sulfoxide, we have modeled the specific interactions between the probe DPP and the solvent dimethyl sulfoxide as dielectric friction since both these interactions are electrostatic in nature.

In TX-100 micelles, however, the rotational diffusion of these probes is described by two reorientation times, τ_{slow} and τ_{fast}. Both the slow and fast components of DPP are significantly longer than the corresponding ones of DMDPP. As in the case of homogeneous solutions, the observed behavior is due to the strong hydrogen bonding interactions between the probe and the ethylene oxide groups of the surfactant units of TX-100 micelles. Another plausible explanation for this observation is the aggregation of DPP. It is a well-known fact that DPP forms aggregates in the solid state due to intermolecular hydrogen bonding.[26,27] But DPP is soluble in solvents, only when it can form hydrogen bonds with them so that the intermolecular hydrogen bonding between the DPP units are broken. On the basis of these arguments, one can eliminate aggregation of DPP as the reason for the observed behavior. Now we turn our attention to the two-exponential anisotropy decay of DMDPP and DPP in TX-100 micelles. Biexponential anisotropy decay of the probes solubilized in micelles is possible if the probes are located in two distinct regions of the micelle, in the core and in the stern layer. These are the only two probable locations as both DMDPP and DPP are nondipolar and are not soluble in

TABLE 1: Temperature Dependence of Fluorescence Lifetimes and Anisotropy Decay Parameters of DMDPP in Triton X-100 Micelles

temp/K	[a]τ_f/ns	r_0	β	τ_{slow}/ns	τ_{fast}/ns	[b]$\langle\tau_r\rangle$/ns	[c]$\langle r\rangle$	[d]$\langle r\rangle$
283	8.81	0.331 ± 0.002	0.69 ± 0.01	6.7 ± 0.4	1.31 ± 0.04	5.03	0.112 ± 0.005	0.126 ± 0.004
288	8.76	0.332 ± 0.003	0.64 ± 0.01	5.6 ± 0.2	1.21 ± 0.01	4.02	0.097 ± 0.004	0.102 ± 0.003
293	8.76	0.341 ± 0.017	0.57 ± 0.03	4.9 ± 0.4	1.11 ± 0.06	3.27	0.09 ± 0.01	0.083 ± 0.002
298	8.74	0.337 ± 0.003	0.53 ± 0.04	4.0 ± 0.3	0.94 ± 0.05	2.56	0.071 ± 0.008	0.063 ± 0.002
303	8.75	0.327 ± 0.011	0.48 ± 0.02	3.4 ± 0.1	0.88 ± 0.12	2.09	0.059 ± 0.007	0.051 ± 0.002
308	8.73	0.323 ± 0.002	0.51 ± 0.06	2.4 ± 0.3	0.73 ± 0.08	1.58	0.048 ± 0.008	0.043 ± 0.001
318	8.72	0.322 ± 0.002	0.48 ± 0.06	1.7 ± 0.2	0.47 ± 0.05	1.06	0.034 ± 0.006	0.028 ± 0.001
323	8.68	0.329 ± 0.004	0.52 ± 0.04	1.2 ± 0.1	0.38 ± 0.02	0.81	0.027 ± 0.004	0.023 ± 0.001

[a] The maximum error in the fluorescence lifetimes is less than 2%. [b] Calculated using eq 4. [c] Calculated from the experimentally measured values of τ_f, τ_{slow}, τ_{fast}, r_0, and β using eq 6. [d] Measured using steady-state depolarization method.

TABLE 2: Temperature Dependence of Fluorescence Lifetimes and Anisotropy Decay Parameters of DPP in Triton X-100 Micelles

temp/K	[a]τ_f/ns	r_0	β	τ_{slow}/ns	τ_{fast}/ns	[b]$\langle\tau_r\rangle$/ns	[c]$\langle r\rangle$	[d]$\langle r\rangle$
283	7.06	0.333 ± 0.003	0.70 ± 0.01	10.9 ± 0.4	2.2 ± 0.2	8.29	0.165 ± 0.007	0.193 ± 0.005
288	6.98	0.336 ± 0.002	0.67 ± 0.01	9.1 ± 0.2	1.64 ± 0.04	6.64	0.148 ± 0.004	0.166 ± 0.003
293	6.99	0.345 ± 0.010	0.63 ± 0.01	7.8 ± 0.2	1.50 ± 0.05	5.47	0.137 ± 0.007	0.144 ± 0.002
298	6.91	0.338 ± 0.001	0.59 ± 0.05	6.4 ± 0.4	1.4 ± 0.1	4.35	0.12 ± 0.01	0.119 ± 0.002
303	6.92	0.348 ± 0.012	0.58 ± 0.03	5.2 ± 0.2	1.06 ± 0.02	3.46	0.106 ± 0.009	0.105 ± 0.002
308	6.90	0.339 ± 0.006	0.55 ± 0.02	4.3 ± 0.1	1.00 ± 0.07	2.82	0.091 ± 0.006	0.089 ± 0.002
318	6.87	0.331 ± 0.001	0.50 ± 0.01	3.4 ± 0.1	0.81 ± 0.05	2.11	0.072 ± 0.003	0.063 ± 0.001
323	6.84	0.336 ± 0.004	0.53 ± 0.05	2.7 ± 0.2	0.62 ± 0.04	1.72	0.064 ± 0.008	0.053 ± 0.002

[a] The maximum error in the fluorescence lifetimes is less than 2%. [b] Calculated using eq 4. [c] Calculated from the experimentally measured values of τ_f, τ_{slow}, τ_{fast}, r_0, and β using eq 6. [d] Measured using steady-state depolarization method.

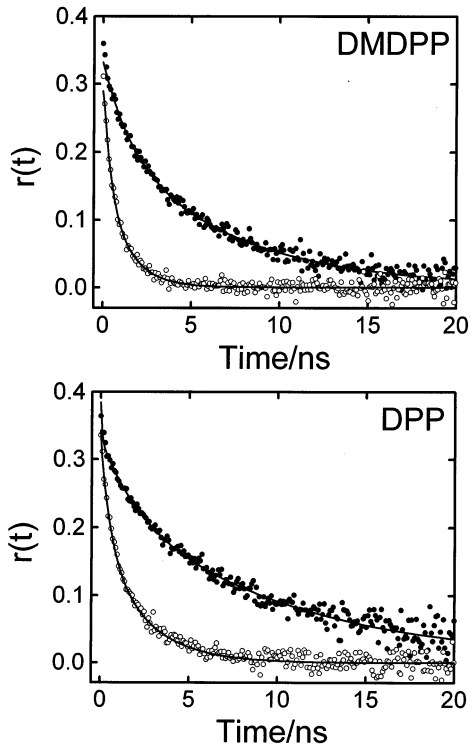

Figure 4. Anisotropy decays of the probes in TX-100 miclles at 283 K (filled circles) and at 323 K (open circles). The lines passing through them are the fitted ones.

water. For this argument to be genuine, a two-exponential fluorescence decay with two lifetimes should have been observed. But on the contrary only one lifetime is observed for each probe, which rules out the possibility that the probes are solubilized in two separate locations. In addition, since DPP is not soluble in alkane-like solvents, it cannot be located in the core of the micelle, which is more like a hydrocarbon solvent.

However, in a recent study, Fayer and co-workers[28] have measured the fluorescence lifetimes of 2-ethylnaphthalene (2EN) in cationic micelles, tetradecyl-trimethylammonium bromide (TTAB), and dodecyl-trimethylammonium bromide (DTAB). They showed that the probe 2EN is dynamically partitioned between the headgroup region and the core region. In other words, the probe is exchanging between the two regions faster than the fluorescence lifetime, resulting in a single-exponential decay. But in our case, as we will show later during the course of the analysis by applying the wobbling in a cone model that the probes DMDPP and DPP are indeed located in the headgroup region of the micelle.

The fast and slow reorientation times can be understood using the two-step model. The two-step model was first introduced to explain the results obtained from nuclear magnetic resonance (NMR) experiments on micelles.[29,30] According to the two-step model, the fast and slow motions are separable and the total correlation function is a product of the two correlation functions corresponding to the fast motion within the micelle and the slow motion of the micelle and is given by[31,32]

$$C_{total}(t) = C_{fast}(t)C_{slow}(t) \tag{7}$$

$C_{slow}(t)$ will decay as single exponential if the slow motion is isotropic and is given by

$$C_{slow}(t) = \exp(-t/\tau_{slow}) \tag{8}$$

NMR relaxation studies[29,30] have shown that τ_{slow} contains contribution from overall rotation of the micelle τ_M and the lateral diffusion τ_L (translational diffusion) of the monomers on the spherical surface of the micelle.

$$\frac{1}{\tau_{slow}} = \frac{1}{\tau_L} + \frac{1}{\tau_M} \tag{9}$$

The fast motion is modeled as restricted rotational diffusion and the correlation function $C_{fast}(t)$ for this motion is given by

$$C_{fast}(t) = (1 - S^2)\exp(-t/\tau_W) + S^2 \tag{10}$$

TABLE 3: Variation of Triton X-100 Micelle Properties with Temperature

temp/K	[a]N_{agg}	[b]r_M/Å	τ_M/ns
283	38	30	38
288	61	37	61
293	54	38	57
298	97	44	77
303	103	49	94
308	137	54	112
318	269	71	204
323	432	83	294

[a] N_{agg} values were read from Figure 5 of ref 12. [b] r_M values were taken from ref 12.

where τ_W is the effective correlation time or reorientation time for wobbling motion of the surfactant that is anchored to the micelle−water interface and this wobbling motion is not isotropic. S is a generalized order parameter, which is a measure of the spatial restriction of the motion. If the motion is isotropic $S = 0$, and if it is completely restricted, $|S| = 1$.

From eqs 7, 8, and 10, the total correlation function can be written as

$$C_{total}(t) = (1 - S^2)\exp(-t/\tau_{fast}) + S^2\exp(-t/\tau_{slow}) \quad (11)$$

where τ_{fast} is given by

$$\frac{1}{\tau_{fast}} = \frac{1}{\tau_W} + \frac{1}{\tau_{slow}} \quad (12)$$

Equation 11 is analogous to eq 3, and hence, the two-step model can be readily adapted to describe the anisotropy decay of the probes in micelles. The two-step model was first applied by Fayer and co-workers[2] to explain the biexponential behavior of merocyanine 540 and octadecylrhodamine B in micelles, and subsequently, it was used by other groups.[3−8]

The time constants for the lateral diffusion of the probe molecules can be obtained from eq 9 if the reorientation time for the overall rotation of the micelle τ_M is known. τ_M can be calculated using the Stokes−Einstein-Debye relation[33] with stick boundary condition.

$$\tau_M = \frac{4\pi r_M^3 \eta}{3kT} \quad (13)$$

where η is the viscosity of water and k and T are the Boltzmann constant and absolute temperature, respectively. r_M is the radius of the micelle. The r_M values and the aggregation numbers of TX-100 micelles as a function of temperature were taken from ref 12 and are given in Table 3. The reorientation times of the micelles that were calculated using eq 13 are also given in the Table. Although the radius of the TX-100 micelles increases only by a factor of 2.8 with a rise in temperature from 283 to 323 K, the τ_M value goes up by a factor of 7.7 because it varies as r_M^3.

The time constants for the lateral diffusion of the probes DMDPP and DPP are given in Tables 4 and 5, respectively. Since the time constants for the overall rotation of the micelles are considerably longer than the τ_{slow} values, τ_{slow} is dominated by lateral diffusion. In fact, at higher temperatures τ_{slow} essentially represents the lateral diffusion of the probes. From the time constants for lateral diffusion one can calculate the lateral diffusion coefficients D_L using the relation[5,7]

$$\tau_L = \frac{r_M^2}{6D_L} \quad (14)$$

TABLE 4: Parameters for the Two-Step Model and Wobbling-in-Cone Model Obtained from Experimental Results for DMDPP

temp/K	τ_L/ns	τ_W/ns	S	θ^o	$D_L \times 10^{10}$/m^2 s^{-1}	$D_W \times 10^{-8}$/s^{-1}
283	8.1	1.63	0.83	28.1	1.9	0.40
288	6.2	1.54	0.80	30.6	3.7	0.49
293	5.4	1.44	0.75	34.6	4.5	0.65
298	4.2	1.23	0.73	36.1	7.7	0.82
303	3.5	1.19	0.69	39.0	11.4	0.97
308	2.5	1.05	0.71	37.6	19.4	1.04
318	1.7	0.65	0.69	39.0	49.4	1.78
323	1.2	0.56	0.72	36.8	95.7	1.87

TABLE 5: Parameters for the Two-Step Model and Wobbling-in-Cone Model Obtained from Experimental Results for DPP

temp/K	τ_L/ns	τ_W/ns	S	θ^o	$D_L \times 10^{10}$/m^2 s^{-1}	$D_W \times 10^{-8}$/s^{-1}
283	15.3	2.76	0.84	27.2	1.0	0.22
288	10.7	2.00	0.82	28.9	2.1	0.34
293	9.0	1.86	0.79	31.4	2.7	0.43
298	7.0	1.79	0.77	33.0	4.6	0.48
303	5.5	1.33	0.76	33.8	7.3	0.68
308	4.5	1.30	0.74	35.4	10.8	0.76
318	3.5	1.06	0.71	37.6	24.0	1.03
323	2.7	0.80	0.73	36.1	42.5	1.27

This process can be viewed as translational diffusion of the probe on the curved surface of the micelle, which is diffusion in three-dimensions. The D_L values obtained using eq 14 are given in Tables 4 and 5 for DMDPP and DPP, respectively. D_L values obtained at 298 K for DMDPP and DPP are comparable to those obtained for other probes in TX-100 micelles.[2,5] DPP diffuses about 2 times slower than DMDPP because it interacts strongly with TX-100 micelles. Also, the D_L values increase by a factor of 50 and 40 for DMDPP and DPP, respectively, as the temperature goes up from 283 to 323 K. This kind of increase cannot be accounted for by the changes in the viscosity and temperature alone. It has been observed in earlier studies[2,5] that, as the size of the micelle increases, τ_L values also increase and the lateral diffusion coefficients for a given probe remain more or less the same, which is consistent with eq 14. However, those studies have been carried out in different types of micelles at room temperature. In the present study, however, the micelle size has been increased by rising the temperature. For an increase in temperature from 283 to 323 K, the viscosity of water decreases from 1.31 to 0.55 mPa s, resulting in the reduction of the η/T value by a factor of 2.7. Since D_L is inversely proportional to η/T, it should increase with an increase in temperature. But even after accounting for the decrease in η/T, the D_L values are increasing by a factor of 19 and 16 for DMDPP and DPP, respectively. The most probable reason for obtaining such high values of D_L could be due to the degree of hydration of TX-100 micelles. The degree of hydration, which is defined as the number of grams of water per gram of TX-100, increases from 1.7 at 283 K to 4.4 at 323 K.[12] In other words, the amount of water associated with each micelle increases with an increase in the temperature. Since the probes used in the present study are hydrophobic in nature, they are pushed inward more toward the stern layer and away from the surface due to the penetration of water molecules in the micelle as a result of increase in the degree of hydration with temperature. Even though the radius of the TX-100 micelle increases with temperature, the exact location of the probe in the micelle also changes with it due to the increase in the degree of hydration of TX-100 micelles. Hence the radius of the surface on which the probes are diffusing is smaller than the actual radius of the micelle. Moreover, the microviscosity experienced

by the probe molecule may also be different, as it is not uniform throughout the micelle.

The information pertinent to wobbling motion is contained in τ_{fast}. According to the wobbling-in-cone model, the probe molecules wobble freely inside a cone of semi angle θ. The relaxation time corresponding to the wobbling motion is obtained from eq 12, and the τ_W values are given in Tables 4 and 5 for DMDPP and DPP, respectively. The order parameter S is obtained using the relation

$$S^2 = \beta \tag{15}$$

The order parameters obtained for DMDPP and DPP are also given in Tables 4 and 5, respectively. The S values are more than 0.8 at lower temperatures and are around 0.7 at higher temperatures for both DMDPP and DPP. These high values for the order parameter indicate that the probes are solubilized near the micelle-water interface, as there is a high degree of order near the interface than in the interior of the micelle. From the order parameter one can obtain θ using the following equation[2]

$$S = \frac{1}{2}\cos\theta\,(1 + \cos\theta) \tag{16}$$

The above relation is valid if the probe molecule is a symmetric ellipsoid and its transition moment is parallel to the long axis. From τ_W, S and θ, the diffusion coefficient for the wobbling motion D_W is obtained using the relation[31,32]

$$D_W = \frac{1}{[(1-S^2)\tau_W]}\left[\frac{x^2(1+x)^2}{2(x-1)}\left\{\ln\left(\frac{(1+x)}{2}\right) + \frac{(1-x)}{2}\right\} + \frac{(1-x)}{24}(6 + 8x - x^2 - 12x^3 - 7x^4)\right] \tag{17}$$

where $x = \cos\theta$. Using eqs 16 and 17, the cone angle and wobbling diffusion coefficients were calculated and are given in Tables 4 and 5, respectively, for DMDPP and DPP. From the Tables it is clear that D_W values increase with temperature, which indicates that the probe molecules become more mobile at higher temperatures. However, unlike the D_L values, the increase in the D_W values can be accounted for by the changes in the viscosity and temperature. As with the case of lateral diffusion coefficients, the wobbling diffusion coefficients are also smaller for DPP compared to DMDPP due to the specific interactions between DPP and TX-100 micelles. It must also be noted that even though the wobbling diffusion coefficient for both the probes at a given temperature is quite different, the wobbling angle θ is almost the same. The θ values obtained for DMDPP and DPP at 298 K are consistent with those obtained by Maiti et al.[5] for a number of probes in TX-100. Since the wobbling angles are determined from the order parameter using eq 16, the more or less identical cone angles for both the probes implies that they are located almost in the same region of the TX-100 micelles.

Another issue we would like to comment on is the reason the rotational dynamics of TX-100 micelles could not be monitored experimentally despite the specific interactions between DPP and TX-100 micelles. It can be explained in the following manner. In order for the rotational dynamics to be effected by the hydrogen bonding interactions, the hydrogen bonding dynamics should take place on a time scale that is comparable to or slower than the rotational dynamics. The rate of the hydrogen bonding dynamics depends on the strength of the hydrogen bonds; if the hydrogen bond strengths are higher the dynamics will be slower and vice versa.[9] In case of DPP and TX-100, these hydrogen bonding interactions are probably not strong enough to effect the dynamics of TX-100 micelles. However, it must be noted that even if these interactions were strong enough, it would not have been possible to measure the micelle reorientation times experimentally because the τ_M values of TX-100 are 5−42 times longer than the fluorescence lifetimes of DPP in TX-100. At the least, however, the experimentally measured steady-state anisotropies would have been close to the r_0 values.

Conclusions

From rotational dynamics studies in homogeneous solutions, it has been fairly well established that specific interactions between the solute and the solvent significantly hinder the solute's rotation. But how the specific interactions between micelles and the probes solubilized in them influence the dynamics of the probe have not been explored. With an intent to find an answer to this question and also how the size of the micelle effects the dynamics of the probe, temperature dependent rotational diffusion studies of two structurally similar nondipolar probes: DMDPP and DPP, have been carried out in TX-100 micelles. The decay of anisotropy for both the probes in TX-100 micelles can be adequately described by two exponential function with a slow reorientation time and a fast one at all the temperatures studied. These results are explained using a two-step model with slow lateral diffusion of the probe on the surface of the micelle and fast wobbling motion of the probe in the micelle, which are coupled to the overall rotation of the micelle. However, it has been observed that when the size of the micelle increases with a rise in temperature, the slow component essentially represents the lateral diffusion of the probe. The lateral diffusion coefficient and the diffusion coefficient for wobbling motion of DPP are found to be considerably smaller than those of DMDPP due to the specific interactions between DPP and TX-100 micelles.

Acknowledgment. I thank my friend the late Dr. V. J. P. Srivatsavoy for a gift of the probes DMDPP and DPP used in this study. I acknowledge the help rendered by Mr. A. S. R. Koti and Mr. V. V. N. Ravi Kishore during the time-resolved fluorescence experiments. I am grateful to Dr. B. S. Valaulikar for useful discussions. I also thank Dr. A. V. Sapre, Dr. T. Mukherjee and Dr. J. P. Mittal for their encouragement throughout the course of this work.

References and Notes

(1) Visser, A. J. W. G.; Vos, K.; Hoek, A. V.; Santems, J. S. *J. Phys. Chem.* **1988**, *92*, 759.

(2) Quitevis, E. L.; Marcus, A. H.; Fayer, M. D. *J. Phys. Chem.* **1993**, *97*, 5762.

(3) Wittouck, N.; Negri, R. M.; Ameloot, M.; De Schryver, F. C. *J. Am. Chem. Soc.* **1994**, *116*, 10601.

(4) Maiti, N. C.; Mazumdar, S.; Periasamy, N. *J. Phys. Chem.* **1995**, *99*, 10708.

(5) Maiti, N. C.; Krishna, M. M. G.; Britto, P. J.; Periasamy, N. *J. Phys. Chem. B* **1997**, *101*, 11051.

(6) Matzinger, S.; Hussey, D. M.; Fayer, M. D. *J. Phys. Chem. B* **1998**, *102*, 7216.

(7) Krishna, M. M. G.; Das, R.; Periasamy, N.; Nityananda, R. *J. Chem. Phys.* **2000**, *112*, 8502.

(8) Sen, S.; Sukul, D.; Dutta, P.; Bhattacharyya, K. *J. Phys. Chem. A* **2001**, *105*, 7495.

(9) Fleming, G. R. *Chemical Applications of Ultrafast Spectroscopy*; Oxford University Press: New York, 1986.

(10) Mukerjee, P.; Cardinal, J. R. *J. Phys. Chem.* **1978**, *82*, 1620.

(11) Ganesh, K. N.; Mitra, P.; Balasubramanian, D. *J. Phys. Chem.* **1982**, *86*, 4291.

(12) Streletzky, K.; Phillies, G. D. J. *Langmuir* **1995**, *11*, 42.

(13) Dutt, G. B.; Srivatsavoy, V. J. P.; Sapre, A. V. *J. Chem. Phys.* **1999**, *110*, 9623.
(14) Dutt, G. B.; Srivatsavoy, V. J. P.; Sapre, A. V. *J. Chem. Phys.* **1999**, *111*, 9705.
(15) Dutt, G. B.; Krishna, G. R. *J. Chem. Phys.* **2000**, *112*, 4676.
(16) Dutt, G. B. *J. Chem. Phys.* **2000**, *113*, 11154.
(17) Dutt, G. B.; Ghanty, T. K. *J. Chem. Phys.* **2002**, *116*, 6687.
(18) O'Connor, D. V.; Phillips, D. *Time-Correlated Single Photon Counting*; Academic Press: London, 1984.
(19) Bevington, P. R. *Data Reduction and Error Analysis for the Physical Sciences*; McGraw-Hill: New York, 1969.
(20) Cross, A. J.; Fleming, G. R. *Biophys. J.* **1984**, *46*, 45.
(21) Knutson, J. R.; Beechem, J. M.; Brand, L. *Chem. Phys. Lett.* **1983**, *102*, 501.
(22) Lackowicz, J. R. *Principles of Fluorescence Spectroscopy*; Plenum Press: New York, 1983.
(23) Brocklehurst, B.; Young, R. N. *J. Phys. Chem. A* **1999**, *103*, 3809.
(24) Gierer, A.; Wirtz, K. *Z. Naturforsch.* **1953**, *A8*, 532.
(25) Dote, J. L.; Kivelson, D.; Schwartz, R. N. *J. Phys. Chem.* **1981**, *85*, 2169.
(26) Adachi, M.; Nakamura, S. *J. Phys. Chem.* **1994**, *98*, 1796.
(27) Srivatsavoy, V. J. P.; Moser, J.-E.; Grätzel, M.; Chassot, L. *J. Colloid Interface Sci.* **1999**, *216*, 189.
(28) Cang, H.; Brace, D. D.; Fayer, M. D. *J. Phys. Chem. B* **2001**, *105* 10007.
(29) Wennerström, H.; Lindman, B.; Söderman, O.; Drakenberg, T.; Rosenholm, J. B. *J. Am. Chem. Soc.* **1979**, *101*, 6860.
(30) Ahläs, T.; Söderman, O.; Hjelm, C.; Lindman, B. *J. Phys. Chem.* **1983**, *87*, 822.
(31) Lipari, G.; Szabo, A. *Biophys. J.* **1980**, *30*, 489.
(32) Lipari, G.; Szabo, A. *J. Am. Chem. Soc.* **1982**, *104*, 4546.
(33) Debye, P. *Polar Molecules*; Dover: New York, 1929.